

Surface and bulk properties of deposits grown with a bidisperse ballistic deposition model

F. A. Silveira* and F. D. A. Aarão Reis†

Instituto de Física, Universidade Federal Fluminense, Avenida Litorânea s/n, 24210-340 Niterói RJ, Brazil

(Received 26 April 2007; published 28 June 2007)

We study roughness scaling of the outer surface and the internal porous structure of deposits generated with the three-dimensional bidisperse ballistic deposition (BBD), in which particles of two sizes are randomly deposited. Systematic extrapolation of roughness and dynamical exponents and the comparison of roughness distributions indicate that the top surface has Kardar-Parisi-Zhang (KPZ) scaling for any ratio F of the flux between large and small particles. A scaling theory predicts the characteristic time of the crossover from random to correlated growth in BBD and provides relations between the amplitudes of roughness scaling and F in the KPZ regime. The porosity of the deposits monotonically increases with F and scales as $F^{1/2}$ for small F , which is also explained by the scaling approach and illustrates the possibility of connecting surface growth rules and bulk properties. The suppression of relaxation mechanisms in BBD enhances the connectivity of the deposits when compared to other ballisticlike models, so that they percolate down to $F \approx 0.05$. The fractal dimension of the internal surface of the percolating deposits is $D_F \approx 2.9$, which is very close to the values in other ballistic-like models and suggests universality among these systems.

DOI: 10.1103/PhysRevE.75.061608

PACS number(s): 81.15.Aa, 68.35.Ct, 68.55.Jk, 81.05.Rm

I. INTRODUCTION

The large number of applications of porous materials and the need to understand and control their properties motivates the proposal of models to represent their geometry and the study of its effects on physical processes taking place in the pore system [1,2]. In some models, the formation of the porous structure is a consequence of a certain growth dynamics which represents its main mechanisms. One example is ballistic deposition (BD), which was originally proposed by Vold to describe sedimentary rock formation [3], and whose growth rules are illustrated in Fig. 1(a). Extensions of this model were already used to produce porous deposits where fluid adsorption and diffusion were studied in connection to the bulk geometry (see, e.g., Ref. [4]). In parallel, surface roughness of ballistic deposits have also attracted much attention [5–13], particularly for the connection with the Kardar-Parisi-Zhang (KPZ) theory [14].

A related model, called bidisperse ballistic deposition (BBD), was recently proposed for sedimentary rock formation. Its growth rules are illustrated in Fig. 1(b). In the three-dimensional version, particles of two different sizes may incident vertically towards the surface: single site particles (size $1 \times 1 \times 1$ in lattice units) with probability $1-F$ and double site particles (size $2 \times 1 \times 1$) with probability F . Any incident particle permanently sticks at the first position where it encounters a previously deposited particle below it. This bimodal distribution of particle size is believed to be realistic because real sand grains are reported to be ellipsoidal with the long axis approximately twice the shortest one [15]. Indeed, there is a large number of simple growth models with two species of particles or two particle orientations which can reproduce real systems features [4,16–20], which justifies the interest in models such as BBD.

Due to its simple stochastic rules, BBD may be useful to connect the growth mechanisms, which depend only on the outer surface properties, and the internal morphology of porous deposits. However, this important question was not addressed in previous work on BBD. In Ref. [15], some properties of the porous deposits were numerically studied, such as porosity and permeability, but detailed information on their connectivity was not provided. In Ref. [21], where only surface roughness scaling was analyzed, it was suggested that the dynamical exponent abruptly changes from the KPZ value for $F > 0.2$ to another value for smaller F (this is typical of a transition between different dynamic growth phases [18]).

This scenario motivates the present work, in which a systematic analysis of surface and bulk properties of the deposits generated by BBD in $2+1$ dimensions will be performed. Our first step is to show that deviations of scaling exponents from the KPZ values are related to a crossover from random to correlated growth, whose characteristic times are very large for small F . This conclusion follows from a scaling approach similar to Refs. [22–24] and will also be confirmed by simulation results. The comparison of scaled roughness distributions of BBD and other KPZ models [25] will pro-

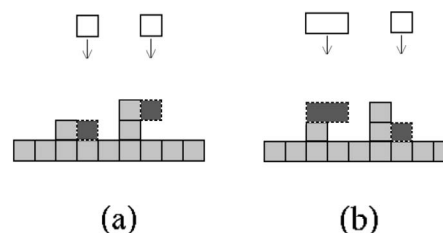


FIG. 1. (a) Growth rules of the original ballistic deposition (BD) model in a line. (b) Growth rules of the bidisperse ballistic deposition (BBD) model in a line. In both cases, aggregated particles are shown in light grey, incident particles in white and aggregation positions of incoming particles in dark grey and with dashed contour.

*fsilveira@if.uff.br

†reis@if.uff.br

vide additional support to the claim that BBD is in the KPZ class for any value of F .

However, surface roughness scaling contains limited information on the structure of the deposit generated by BBD because it only takes into account the correlations of the heights of the highest particles of each column of the deposit, i.e., of the outer surface. We will show that the pore system below this surface has a high connectivity (i.e., the system of pores percolates) in an exceptionally large range of values of F , from $F=1$ down to $F \approx 0.05$, so that the internal surface of the deposit has a fractal dimension as large as $D_F \approx 2.9$. This value is very close to D_F for the original BD model and for an extension of BD including relaxation [26], which suggests universality of the surface fractal dimension among a large class of ballisticlike deposits.

In addition, we will illustrate the possibility to connect the internal properties of the deposit with growth rules (the particle size distribution and the parameter F) by extending our scaling arguments to show that the porosity of the deposits scales as $F^{1/2}$ for small F . Only a small number of recent works was devoted to the simultaneous study of bulk and surface properties in growth models [26–28], but such studies are certainly very important for a realistic modelling of growth of porous media.

The rest of this paper is organized as follows. In Sec. II we present estimates of roughness and dynamical exponents for the BBD and compare numerically calculated roughness distributions in the steady states. In Sec. III we present a scaling theory that explains the crossover from random to KPZ growth in the BBD model, with the relative flux F being the control parameter of this crossover. In Sec. IV we analyze the porosity of the deposits. In Sec. V we study the connectivity of the deposits and the scaling properties of the internal surface. In Sec. VI we summarize our results and discuss possible applications and extensions of the present work.

II. NUMERICAL STUDY OF ROUGHNESS SCALING

In surface growth models, the roughness W is usually defined as the rms fluctuation of the height h around its average position \bar{h} :

$$W(L, t) \equiv [\langle (h - \bar{h})^2 \rangle]^{1/2}, \quad (1)$$

where the overbars indicate spatial averages and the angular brackets indicate configurational averages. In models with pore formation, such as BD and BBD, many particles at each substrate column may be in contact with the external media, thus the interface of the solid phase is multivalued. However, in the definition of the roughness W , the height h of each column is chosen as the height of the highest particle in that column. Thus, W characterizes the outer surface of the deposit, which may be accessible through surface imaging methods and whose scaling properties may be useful for many applications [29].

The above defined roughness certainly do not represent the properties of the porous media, which has a much more complex internal surface, to be studied in Secs. IV and V. In

systems with multivalued interfaces and anomalous scaling of W (which is not the case of BBD), it may even be difficult to characterize the surface properly by calculating this quantity—see, e.g., Ref. [30].

In a random, uncorrelated growth, the roughness increases as

$$W_{\text{random}} \sim t^{1/2}. \quad (2)$$

This is the case of the BBD with $F=0$, in which the deposition in a given column is independent of the neighboring ones. However, in correlated growth processes, the roughness is expected to obey the Family-Vicsek scaling relation [31]

$$W(L, t) \approx AL^\alpha f\left(\frac{t}{t_\times}\right), \quad (3)$$

where L is the system size, α is the roughness exponent, A is a model-dependent constant, f is a scaling function such that $f \sim 1$ in the regime of roughness saturation ($t \rightarrow \infty$), and t_\times is the characteristic time of crossover to saturation. t_\times scales with the system size as

$$t_\times \approx BL^z, \quad (4)$$

where z is the dynamic exponent and B is another model-dependent amplitude. For $t \ll t_\times$ (after a possible crossover to correlated growth), the roughness scales as

$$W \approx Ct^\beta, \quad (5)$$

where C is also model dependent and $\beta = \alpha/z$ is the growth exponent. In this growth regime, $f(x) \sim x^\beta$ in Eq. (3). In most limited-mobility growth models (i.e., models without collective diffusion), the time unit is taken as the time necessary to deposit the mass of one monolayer.

The rms fluctuation of the squared roughness in the steady state is

$$\sigma \equiv \sqrt{\langle w_2^2 \rangle - \langle w_2 \rangle^2}, \quad (6)$$

where $w_2 \equiv \bar{h}^2 - \bar{h}^2$ indicates the roughness of a given configuration. σ scales with the same exponents of W multiplied by 2, but with much weaker finite-size corrections, as previously shown for some growth models in Ref. [25]. Thus, here we will use σ instead of W for estimating roughness and dynamical exponents.

We simulated the BBD model for several values of F , ranging from $F=0.06$ to $F=0.40$, in two-dimensional substrates of linear sizes L ranging from $L=16$ to $L=512$, up to the steady states. Nearly 10^4 configurations were simulated for each F and L .

Effective roughness exponents are defined as

$$\alpha(L) \equiv \frac{1}{2} \frac{\ln[\sigma_{\text{sat}}(L)/\sigma_{\text{sat}}(L/2)]}{\ln 2}, \quad (7)$$

where $\sigma_{\text{sat}}(L)$ stands for the rms fluctuation of the squared saturation roughness (i.e., steady state roughness) of a system of size L . In Fig. 2(a) we show the effective exponents $\alpha(L)$ as a function of $1/L$ for $F=0.08$. Extrapolation to $L \rightarrow \infty$ gives $\alpha=0.395$. The variable in the abscissa was shown

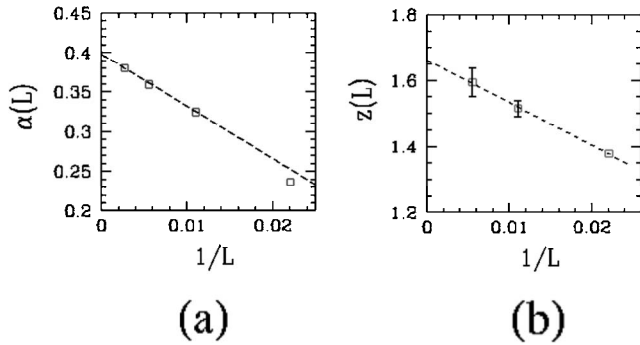


FIG. 2. (a) Effective roughness exponents versus inverse lattice size for BBD with $F=0.08$. The linear fit of the data for $64 \leq L \leq 512$ (dashed line) gives $\alpha \sim 0.395$. (b) Effective dynamic exponents versus inverse lattice size for BBD with $F=0.1$. The linear fit of the data for the largest lattice sizes (dashed line) gives $z \sim 1.66$. Where error bars are not shown, they are smaller than the data points.

to provide a good linear fit of the large L data among other integer and half-integer powers of L . A more refined extrapolation procedure, similar to Ref. [32], gives nearly the same value of α as $L \rightarrow \infty$.

The value $F=0.08$ in Fig. 2(a) is in the region where KPZ scaling was not observed in previous work [21]. However, the extrapolated α is in excellent agreement with the best known estimates for the KPZ class in $d=2+1$ dimensions, which are in the range $[0.375, 0.396]$ [32]. Our estimates of α for all values of F , from 0.06 to 0.40, are also consistent with the KPZ range.

We also calculated characteristic times $\tau(L)$ which are proportional to the saturation times t_\times [Eqs. (3) and (4)], using the method introduced in Ref. [33]. Effective exponents z are defined as

$$z(L) \equiv \frac{\ln[\tau(L)/\tau(L/2)]}{\ln 2}. \quad (8)$$

In Fig. 2(b) we plot $z(L)$ as a function of $1/L$ for $F=0.1$, which gives $z=1.66 \pm 0.05$ asymptotically. This value of F is also in the region where Ref. [21] did not find KPZ scaling. However, the above estimate also has an intersection with the best previous estimate of z for the KPZ class, in the range $[1.605, 1.64]$ [32]. For the other values of F , the estimates of z also intercept this KPZ range.

Additional support to the claim that BBD has KPZ scaling follows from comparison of distributions of the squared width $w_2 \equiv \bar{h}^2 - \bar{h}^2$ in the steady state. Letting $P(w_2)$ be the probability density of the roughness of a given configuration to lie in the range $[w_2, w_2 + dw_2]$, it is expected that this density satisfies the scaling relation $P(w_2) = \frac{1}{\sigma} \Psi\left(\frac{w_2 - \langle w_2 \rangle}{\sigma}\right)$, with σ defined above and Ψ being a universal function (see, e.g., Ref. [34]). In Fig. 3 we plot the steady state scaled distributions for the BBD model with $F=0.06$ and $F=0.1$ and for the restricted solid-on-solid (RSOS) model, which is one of the best representatives of the KPZ class. The good collapse of the curves for the different models indicates that BBD is in

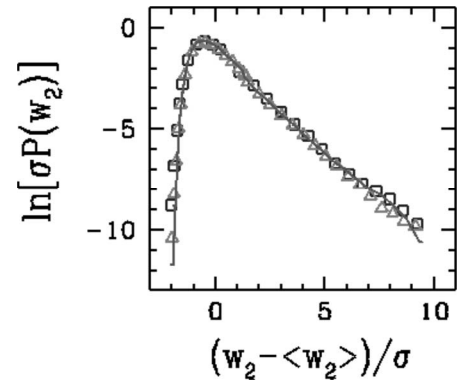


FIG. 3. Steady state scaled roughness distributions for the BBD model with $F=0.06$ (triangles) and $F=0.10$ (squares) and for the RSOS model (solid curve).

the KPZ class in $2+1$ dimensions for all values of F . Quantitatively, the collapse of the curves is confirmed by the values of the skewness S and of the kurtosis Q : for BBD with $F=0.06$ we have $S=1.70 \pm 0.02$ and $Q=5.50 \pm 0.20$, for BBD with $F=0.1$ we have $S=1.69 \pm 0.02$ and $Q=5.42 \pm 0.20$, and for the RSOS model we have $S=1.71 \pm 0.02$ and $Q=5.4 \pm 0.1$ [25].

III. SCALING THEORY FOR THE CROSSOVER OF SURFACE ROUGHNESS

In order to provide an explanation for the deviations in the roughness scaling of BBD observed in previous works, now we analyze its scaling properties along the same lines of other competitive models [22–24]. This approach will also be useful to explain the scaling of the porosity for small F in Sec. IV.

In BBD with high fluxes of large particles ($F \leq 1$), the ballisticlike nature of the problem is clear and the KPZ scaling was shown in early simulation work [21]. On the other hand, with small F , most deposition attempts (of small particles) lead to uncorrelated growth. However, as shown in Fig. 1, a single deposition of a large particle (whose long axis is oriented in one of the surface directions) always leads to the same final height in two neighboring columns. The aggregation of this particle immediately introduces correlations among those columns. The typical time interval for deposition of this particle in a given column is $1/F$, which is large when F is small, while that typical time is of order unity for $F \approx 1$. Consequently, we expect that the same features of the model with $F \approx 1$ will be present in the model with small F , but with all characteristic times rescaled by a factor $1/F$.

The constant B in Eq. (4) is of order 1 for the model with $F \approx 1$, as well as in the original BD model (see, e.g., Ref. [33]). Thus, in BBD with small F , we expect that

$$B \sim 1/F. \quad (9)$$

Now consider a narrow system, i.e., with lattice size L of order unity. The columns inside this system randomly grow

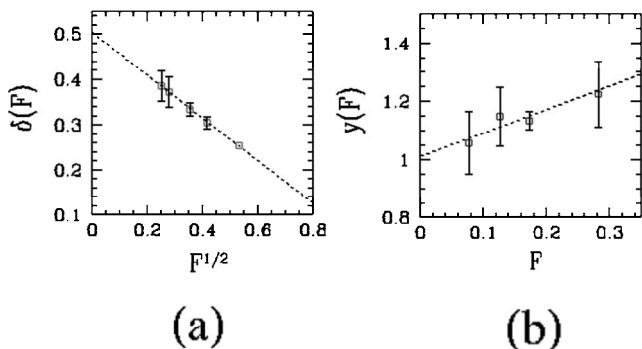


FIG. 4. (a) Effective exponent $\delta(F)$ as a function of $F^{1/2}$ and a linear fit (dashed line) which gives $\delta=0.50\pm0.02$ as $F\rightarrow 0$. (b) Effective exponent $y(F)$ as a function of F and a linear fit (dashed line) which gives $y=1.01\pm0.10$ as $F\rightarrow 0$.

until a time of order $1/F$. During this time interval, the roughness increases as in random deposition [Eq. (2)]. Thus, at $t\sim 1/F$, the roughness is of order $(1/F)^{1/2}$. When a small number of correlated depositions occurs, the whole (small) system will be correlated and the roughness will saturate at a value of this order of magnitude. This means that the amplitude in Eq. (3) must scale as

$$A \sim 1/F^{1/2} \tag{10}$$

in BBD with small F . Combined with this result, FV scaling and Eq. (5) immediately lead to $C\sim 1/F^{1/2-\beta}$, with the KPZ exponent β .

The above discussion shows that deviations from KPZ scaling in BBD with small F are just finite-time or finite-size effects due to long crossovers from random to correlated growth. In order to test this scaling approach, we estimated the amplitudes A and B in the limit $L\rightarrow\infty$ by extrapolating the ratios $W_{\text{sat}}(L)/L^\alpha$ and $\tau(L)/L^z$, respectively. The values $\alpha=0.385$ and $z=1.615$ of the KPZ class [32] were used in the calculation of those quantities. Following the notation of Ref. [35], we assume that

$$A \sim F^{-\delta} \tag{11}$$

and

$$B \sim F^{-\gamma}. \tag{12}$$

Effective exponents for δ and γ were calculated as

$$\delta(F) \equiv -\frac{\ln[A(F'')/A(F')]}{\ln(F''/F')}, \tag{13}$$

$$y(F) \equiv -\frac{\ln[B(F'')/B(F')]}{\ln(F''/F')}, \tag{14}$$

with $F=\sqrt{F''F'}$ and successive values F', F'' . In Figs. 4(a) and 4(b) we show $\delta(F)$ and $y(F)$ as functions of $F^{1/2}$ and F , respectively, and linear extrapolations of the data for small F . Again, the variables in the abscissas were chosen to provide good linear fits of the low F data. The extrapolations to $F\rightarrow 0$ give exponents consistent with the values $\delta=1/2$ and

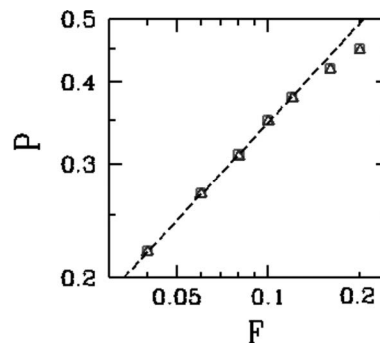


FIG. 5. Porosity P versus F for BBD in substrate sizes $L=256$ (squares) and $L=128$ (triangles). The linear fit of the data for $F\leq 0.1$ (dashed line) has slope 0.503 ± 0.003 .

$y=1$ predicted in Eqs. (10) and (9), respectively, thus confirming the validity of our scaling approach.

IV. POROSITY OF THE DEPOSITS

Now we begin the analysis of the internal structure of the deposits. The simplest quantity to characterize a porous structure is the porosity P , which is the fraction of empty lattice sites inside the deposit. In Fig. 5 we show a log-log plot of P as a function of F . Results for different substrate sizes confirm the absence of significant finite-size effects. As F increases towards $F=1$, P tends to saturate, as expected. However, for small P , a fit of our data gives

$$P \sim F^a, \tag{15}$$

with a numerical estimate $a=0.503\pm 0.003$ obtained from the data for $L=256$. This result contrasts to the exponent $a=0.63$ obtained in Ref. [15] in 2+1 dimensions (in that work, the exponent $a\approx 0.5$ was obtained in 1+1 dimensions).

It is possible to extend the scaling arguments of Sec. III to explain why $a=1/2$ for BBD in all dimensions. As discussed above, the correlation between columns is produced by the incidence of large particles at time intervals of order $1/F$, for small F , and the random growth leads to a typical height difference between neighboring columns of order $1/F^{1/2}$. Thus, when a large particle is deposited, it will typically create a pore with height of order $1/F^{1/2}$ and with lateral size of order unity. This is confirmed in Figs. 6(a) and 6(b), where we show cross sections of deposits with $F=1$ and $F=0.2$: for

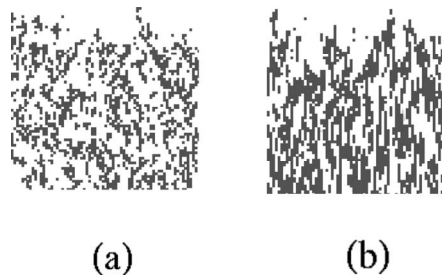


FIG. 6. Cross sectional view of three-dimensional BBD deposits generated with (a) $F=1$ and (b) $F=0.20$.

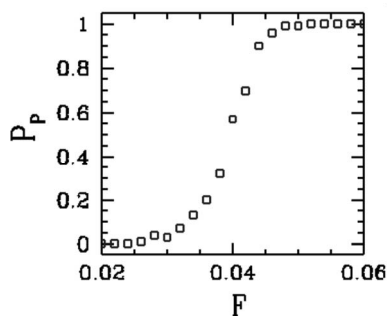


FIG. 7. Percolation probability P_p versus F for the BBD model in substrate sizes $L=256$, which indicates a percolation transition at $F_c \approx 0.04$.

the smaller value of F [Fig. 6(b)], the pores are narrow in the horizontal direction, but vertically high. The overall balance for small F is that an empty volume of order $1/F^{1/2}$ is produced during a time interval in which $1/F$ solid particles are deposited. Consequently, the porosity is expected to be

$$P = V_{\text{pore}} / (V_{\text{solid}} + V_{\text{pore}}) \sim (1/F^{1/2}) / (1/F + 1/F^{1/2}) \sim F^{1/2}, \quad (16)$$

which gives $a=1/2$. Since this argument is based on random deposition properties and the stochastic rules of BBD, it is valid in all substrate dimensions.

The above approach is interesting because it shows that the properties of the surface of the deposit, which depend on the particular growth rules of the model, can be used to determine scaling properties of the porous media below it. A more refined approach was recently used to calculate density-density correlations in the original BD model [27], which also illustrate the possibility of connecting surface and bulk properties. These results may motivate the related studies in systems with more complex growth dynamics.

V. CONNECTIVITY AND FRACTAL DIMENSION OF THE PORE SYSTEM

An interesting property of the deposits generated by BBD is the fact that they have a highly connected pore structure even for relatively small values of the flux of large particles, which are responsible for the formation of pores. This is illustrated in Fig. 6(b), where the deposit with $F=0.2$ still shows a high connectivity of the internal pore system.

In order to decide whether the internal pore system percolates (i.e., it is connected from the substrate up to the external surface), we had to generate relatively small deposits due to memory restrictions. For substrates of linear size $L=256$, we typically deposited 150 monolayers of particles, which may lead to average heights of the deposits near 500 units. Despite these limitations, we were able to observe the transition from an open (percolating) pore structure to a structure of isolated (closed) pores in a narrow region of the parameter F . Figure 7 shows the probability of percolation P_p as a function of F , which indicates a percolation transition at $F_c=0.040 \pm 0.005$. In the limit of infinitely large system sizes, this probability is expected to be a step function

with discontinuity at F_c , since it is the probability that a given configuration percolates (P_p must not be confused with the order parameter of a percolation problem, which is defined as the fraction of the pores belonging to the percolating cluster and which continuously decrease to zero at F_c).

The percolation transition in BBD deposits takes place for porosities between 20% and 25% (see Fig. 6). This is slightly below the critical probability of percolation with randomly distributed vacancies in a simple cubic lattice, $p_c=0.3116$ [36]—in that case, this probability is equal to the porosity. On the other hand, those porosities are still much higher than the ones obtained at the percolation transitions in grain consolidation models, which are close to 0.03 [37]. Those models do not account for particle deposition processes, but lead the formation of narrow channels in a very compact structure by allowing the expansion of internal grains.

In Ref. [26], the properties of the internal and the external surface of porous deposits produced by BD were studied. In the three-dimensional case [(2+1)-dimensional growth], the deposits grown with a model where a fraction of the incident particles could relax after deposition were also studied. Compact layers were obtained for $p < 0.35$, where p is the probability that the incident particle diffuses to a smaller neighboring column, while $1-p$ is the probability of aggregation according to the rules of the original BD model. Low values of porosity (of order 20%) were also obtained near the percolation threshold there. However, the most important conclusion that can be drawn from comparison of these models is that the suppression of relaxation mechanisms have a drastic effect in increasing the pore connectivity if lateral aggregation takes place with low rate, which is the case of BBD with small F .

Now we analyze the properties of the set of surface sites, which are defined as the sites of the deposit which have at least one nearest neighbor belonging to the percolating pore system. This set may be viewed as the internal surface of the pore structure. The total surface area is expected to scale with the coverage θ (number of deposited monolayers) as [26]

$$S \sim L^2 \theta^{D_F - D}, \quad (17)$$

where D_F is the fractal dimension of the internal surface and $D=2$ is the substrate dimension.

In Fig. 8 we show $\ln(S\theta^2/L^2)$ versus $\ln \theta$ for BBD with $F=0.1$ and $F=0.6$. In both cases we obtain $D_F \approx 2.9$ (smaller error bars are near 3% for $F \sim 0.1$). This fractal dimension is the same obtained in deposits generated with the original BD model and with the model including relaxation in Ref. [26]. It strongly suggests universality of D_F among ballistic deposition models in two-dimensional deposits. Again, these numerical findings may be viewed as motivation for further theoretical investigation of the relations between surface growth and bulk properties.

VI. SUMMARY AND CONCLUSION

We studied the surface roughness scaling in the bidisperse ballistic deposition (BBD) model in 2+1 dimensions and the properties of the pore system in the deposits generated with that model.

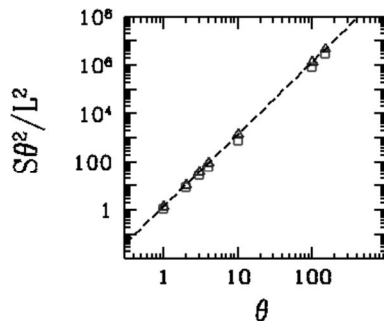


FIG. 8. Scaled surface fractal dimension as a function of coverage in the BBD model with $F=0.1$ (squares) and $F=0.6$ (triangles). The linear fits of the data in the scaling regions (dashed line) give $D_F \approx 2.9$ in both cases.

Systematic extrapolation of roughness and dynamical exponents obtained from simulation in a range of system sizes showed that it presents KPZ scaling for fluxes of large particles $F \geq 0.1$. The values of F analyzed here include the region where previous work suggested a transition in roughness scaling. Comparison of roughness distributions provided additional support to the conclusion that the model is in the KPZ class for all values of F . A scaling approach was used to predict the characteristic time of the crossover from random to correlated growth in BBD and provided relations between scaling amplitudes and F in the KPZ scaling regime. The theoretically predicted crossover exponents were also confirmed by simulation. This scenario rules out the possibility of a roughening transition in BBD.

The porosities P of the deposits generated with BBD were measured for various values of F and it was shown that, for small F , it increases as $P \sim F^{1/2}$. This result is explained with an extension of the previous scaling approach. The deposits have high connectivities in a large range of values of F , down to $F \approx 0.05$. The comparison with ballisticlike models involving surface relaxation show that the suppression of relaxation significantly enhances the connectivity of the pore system for low rates of lateral aggregation. The fractal dimension of the internal surface of the percolating deposits is $D_F \approx 2.9$, which is very close to previously studied ballistic-

like models, thus suggesting universality among these systems.

Concerning roughness scaling, the comparison of former results on BBD [21] and our work illustrates the typical difficulties involved in finding dynamical transitions in growth models and the relevance of theoretical approaches which can provide a deeper insight into the system behavior, even if only in a qualitative way. On the other hand, this study confirms that systematic methods to extrapolate simulation data from finite systems can be very helpful tools.

Concerning bulk features, we believe that our results strongly motivates further theoretical investigation on relations between surface growth rules and internal properties of the deposits. Since simple arguments are capable of explaining the scaling of quantities such as the porosity in a restricted range of the model parameters, it is expected that more sophisticated approaches will be able to address the same question in more complex systems, such as done in Ref. [27]. Moreover, the apparently universal surface fractal dimension of ballisticlike deposits is another important point for further investigation and suggests possible applications of this class of growth model. Indeed, the estimate $D_F=2.9$ is very close to the value $D_F \approx 2.85$ obtained experimentally in sandstones [38,39], and not very far from $D_F=2.7-2.8$ obtained in gold vapor deposition [40]. Another interesting question is what happens in ballisticlike models with varying angles of deposition, which have been recently applied to growth of silicon or silicon compounds [41-43].

Our conclusions also confirm the relevance of BBD as a simplified but realistic model for sedimentary rock formation, as originally proposed in Ref. [15]. In order to provide a quantitative description of real systems, this type of model may eventually include mechanisms such as those of the grain consolidation models [37], which allow the expansion of internal grains, as well as the aggregation of different grain sizes.

ACKNOWLEDGMENTS

F.A.S. acknowledges support from CNPq and F.D.A.A.R. acknowledges support from CNPq and FAPERJ (Brazilian agencies).

-
- [1] R. Hilfer, in *Advances in Chemical Physics*, edited by I. Prigogine and S. A. Rice (Wiley, Chichester, UK, 1996), Vol. XCII.
- [2] M. Sahimi, *Rev. Mod. Phys.* **65**, 1393 (1993).
- [3] M. J. Vold, *J. Colloid Sci.* **14**, 168 (1959); *J. Phys. Chem.* **63**, 1608 (1959).
- [4] M. E. Kainourgiakis, T. A. Steriotis, E. S. Kikkinides, G. Romanos, and A. K. Stubos, *Colloids Surf., A* **206**, 321 (2002); E. S. Kikkinides, K. A. Stoitsas, and V. T. Zaspalis, *J. Colloid Interface Sci.* **259**, 322 (2003).
- [5] P. Meakin, P. Ramanlal, L. M. Sander, and R. C. Ball, *Phys. Rev. A* **34**, 5091 (1986).
- [6] R. Baiod, D. Kessler, P. Ramanlal, L. Sander, and R. Savit, *Phys. Rev. A* **38**, 3672 (1988).
- [7] R. M. D'Souza, Y. Bar-Yam, and M. Kardar, *Phys. Rev. E* **57**, 5044 (1998).
- [8] F. D. A. Aarão Reis, *Phys. Rev. E* **63**, 056116 (2001).
- [9] E. Katzav and M. Schwartz, *Phys. Rev. E* **70**, 061608 (2004).
- [10] D. Rodríguez-Pérez, J. L. Castillo, and J. C. Antoranz, *Phys. Rev. E* **72**, 021403 (2005).
- [11] C. A. Haselwandter and D. D. Vvedensky, *Phys. Rev. E* **73**, 040101(R) (2006).
- [12] J. Desbois, *J. Phys. A* **34**, 1959 (2001).
- [13] F. Hivert, S. Nechaev, G. Oshanin, and O. Vasilyev, *J. Stat. Phys.* **126**, 243 (2007).
- [14] M. Kardar, G. Parisi, and Y.-C. Zhang, *Phys. Rev. Lett.* **56**,

- 889 (1986).
- [15] S. Tarafdar and S. Roy, *Physica B* **254**, 28 (1998).
- [16] E. Guyon, L. Oger, and T. J. Plona, *J. Phys. D* **20**, 1637 (1987).
- [17] E. Caglioti, V. Loreto, H. J. Herrmann, and M. Nicodemi, *Phys. Rev. Lett.* **79**, 1575 (1997).
- [18] F. D. A. Aarão Reis, *Phys. Rev. E* **66**, 027101 (2002).
- [19] J. Mairesse and L. Vuillon, *Theor. Comput. Sci.* **270**, 525 (2002).
- [20] K. Trojan and M. Ausloos, *Physica A* **326**, 492 (2003).
- [21] R. Karmakar, T. Dutta, N. Lebovka, and S. Tarafdar, *Physica A* **348**, 236 (2005).
- [22] F. D. A. Aarão Reis, *Phys. Rev. E* **73**, 021605 (2006).
- [23] C. M. Horowitz and E. V. Albano, *Phys. Rev. E* **73**, 031111 (2006).
- [24] L. A. Braunstein and C.-H. Lam, *Phys. Rev. E* **72**, 026128 (2005).
- [25] F. D. A. Aarão Reis, *Physica A* **364**, 190 (2006).
- [26] J. Yu and J. G. Amar, *Phys. Rev. E* **65**, 060601(R) (2002).
- [27] E. Katzav, S. F. Edwards, and M. Schwartz, *Europhys. Lett.* **75**, 29 (2006).
- [28] J. Yu and J. G. Amar, *Phys. Rev. E* **66**, 021603(R) (2002).
- [29] A. L. Barabási and H. E. Stanley, *Fractal Concepts in Surface Growth* (Cambridge University Press, Cambridge, England, 1995).
- [30] A. Brú and D. Casero, *Europhys. Lett.* **64**, 620 (2003).
- [31] F. Family and T. Vicsek, *J. Phys. A* **18**, L75 (1985).
- [32] E. Marinari, A. Pagnani, and G. Parisi, *J. Phys. A* **33**, 8181 (2000); F. D. A. Aarão Reis, *Phys. Rev. E* **69**, 021610 (2004).
- [33] F. D. A. A. Reis, *Physica A* **316**, 250 (2002).
- [34] T. Antal, M. Droz, G. Györgyi, and Z. Rácz, *Phys. Rev. E* **65**, 046140 (2002).
- [35] C. M. Horowitz, R. A. Monetti, and E. V. Albano, *Phys. Rev. E* **63**, 066132 (2001); C. M. Horowitz and E. Albano, *J. Phys. A* **34**, 357 (2001).
- [36] D. Stauffer and A. Aharony, *Introduction to Percolation Theory*, 2nd ed. (Taylor and Francis, London, 1982).
- [37] J. N. Roberts and L. M. Schwartz, *Phys. Rev. B* **31**, 5990 (1985).
- [38] C. E. Krohn and A. H. Thompson, *Phys. Rev. B* **33**, 6366 (1986).
- [39] A. P. Radlinski, E. Z. Radlinska, M. Agamalian, G. D. Wignall, P. Lindner, and O. G. Randl, *Phys. Rev. Lett.* **82**, 3078 (1999).
- [40] J. M. Gomez-Rodriguez, A. Asenjo, R. C. Salvarezza, and A. M. Baro, *Ultramicroscopy* **42-44**, 1321 (1992).
- [41] S. W. Levine, J. R. Engstrom, and P. Clancy, *Surf. Sci.* **401**, 112 (1998).
- [42] A. Yanguas-Gil, J. Cotrino, A. Barranco, and A. R. González-Elipe, *Phys. Rev. Lett.* **96**, 236101 (2006).
- [43] D.-X. Ye and T.-M. Lu, *Phys. Rev. B* **75**, 115420 (2007).